28. C.-Y. Wang, M. W. Mayo, R. G. Korneluk, D. V. Goeddel, A. S. Baldwin Jr., *Science* **281**, 1680 (1998).
29. G. Zhou, Z. Q. Bao, J. E. Dixon, *J. Biol. Chem.* **270**, 12665 (1995).
30. pGEX-2T-MKK4/SEK1 was a generous gift from J. Woodgett; pGEX2T-MKK3 was a generous gift from T. Sugimoto and K.-L. Guan.
31. C. F. Zheng and K. L. Guan, *J. Biol. Chem.* **269**, 19947 (1994).
32. We thank C. Worby, J. Clemens, T. Maehama, M. Muda, S. Juris, I. Jones, C. Figueroa, and other members of the Dixon lab for stimulating discussions and technical support. We are very grateful to A. Vojtek, K.-L. Guan, Z. Xu, and members of their lab for their generous support and assistance. In addition, we are grateful to A. Lin, J. Woodgett, and M. Cobb for their generous supply of reagents. This work was funded by NIH grants 18024 (J.E.D.) and AI35175 (J.B.B.) and the Walther Cancer Institute (J.E.D. and K.O.).

13 May 1999; accepted 19 August 1999

# Synergy Between Tumor Suppressor *APC* and the β-Catenin–Tcf4 Target *Tcf1*

**Jeroen Roose,[1]* Gerwin Huls,[1]* Moniek van Beest,[1]* Petra Moerer,[1] Karin van der Horn,[1] Roel Goldschmeding,[3] Ton Logtenberg,[1] Hans Clevers[1,2]†**

Mutations in APC or β-catenin inappropriately activate the transcription factor Tcf4, thereby transforming intestinal epithelial cells. Here it is shown that one of the target genes of Tcf4 in epithelial cells is *Tcf1*. The most abundant Tcf1 isoforms lack a β-catenin interaction domain. *Tcf1*$^{-/-}$ mice develop adenomas in the gut and mammary glands. Introduction of a mutant APC allele into these mice substantially increases the number of these adenomas. Tcf1 may act as a feedback repressor of β-catenin–Tcf4 target genes and thus may cooperate with APC to suppress malignant transformation of epithelial cells.

The tumor suppressor gene *APC*, first identified in a dominantly inherited disorder termed familial adenomatous polyposis, is mutated in the vast majority of colorectal cancers (*1*). APC's principal role is that of a negative regulator of the Wnt signal transduction cascade (*2*). APC resides in a large complex with axin, GSK3, and the Wnt effector β-catenin (*3*). In this complex, the serine kinase GSK-3β constitutively phosphorylates β-catenin at a set of regulatory $NH_2$-terminal Ser/Thr residues, thereby targeting β-catenin for ubiquitination by β-TrCP and for subsequent proteasomal degradation (*4*). Wnt signaling stabilizes β-catenin. In the nucleus, β-catenin binds to Tcf/Lef transcription factors. The bipartite complex then activates transcription of Tcf target genes (*5*). In the absence of signaling, Tcf factors repress transcription by interaction with Groucho transcriptional repressors or with CBP (*6*).

Loss of *APC* leads to the nuclear accumulation of β-catenin, which constitutively binds to Tcf4 (*7*), a Tcf family member specifically expressed in epithelia of the intestine and mammary gland (*8*). In some colorectal cancers that carry wild-type *APC* as well as in several other types of cancer, dominant mutations alter one of the four regulatory $NH_2$-terminal Ser/Thr residues of β-catenin. This also leads to the inappropriate formation of β-catenin–Tcf complexes in the nucleus (*9*).

Expression of *Tcf1*, a gene encoding another Tcf family member, is largely restricted to T lineage lymphocytes in adult tissues and cell lines (*10*). However, colorectal cell lines have also been reported to express appreciable amounts of *Tcf1* (*11*). Confirming the latter observation, we detected *Tcf1* mRNA by Northern (RNA) blot analysis in five of six colorectal cell lines (*12*). Three of these are *APC* mutants (SW480, HT-29, and DLD1), and two others (LS174T and HCT116), carry oncogenic mutations in β-catenin. The cell line that did not express *Tcf1* (RKO) is wild-type for both *APC* and β-catenin, suggesting that *Tcf1* expression might normally be regulated by these genes. We also detected nuclear Tcf1 protein in normal human tissues: in proliferating intestinal epithelial cells and in the basal epithelial cells of mammary gland epithelium (*13*) (Fig. 1). The most abundant Tcf1 isoforms lack a β-catenin interaction domain (*10*). Because they retain their Groucho interaction domain, they are likely to act as negative regulators of Wnt signaling.

To test whether *Tcf1* is a target of Tcf4, we used a transfectant derived from the APC$^{-/-}$ HT29 cell line, which inducibly expresses wild-type APC (*14*). This transfectant previously allowed the identification of another Tcf4 target, c-*Myc* (*15*). APC expression was induced in HT29-APC cells for 20 hours. The cells remained attached and were >95% viable. Northern (RNA) blot analysis revealed a consistent four- to fivefold decrease in steady-state mRNA levels for *Tcf1* and c-*Myc* (Fig. 2A), but no changes in the levels of *Ep-Cam* and γ-*actin* mRNAs. This experiment indicated that *Tcf1* is regulated by APC, and therefore by β-catenin–Tcf4.

The human *Tcf1* gene is transcribed from two closely spaced promoters (*10*). We sequenced 1.2 kb directly upstream of promoter I and found the region to be a CpG island containing two potential Tcf-binding motifs (Fig. 2B). The region acted as an enhancer, both in the context of promoter I and of a heterologous promoter (*12*). We tested the inducibility of the putative enhancer fragment by β-catenin and Tcf expression constructs in our "model" B cell line IIA1.6, which lacks endogenous Tcf/Lef factors (*7*, *16*). The combination of β-catenin and Tcf4 transactivated the enhancer three- to fourfold in a transient reporter assay (Fig. 2C). Furthermore, expression of a dominant-negative Tcf4 (ΔNTcf4, which lacks the β-catenin interaction domain) inhibited enhancer activity in LS174T colorectal cancer cells (Fig. 2D).

Tcf1-deficient mice develop a progressive block in early thymocyte development (*17*). Nevertheless, *Tcf1*$^{-/-}$ mice have functional peripheral T cells, are fully immunocompetent, and live for over a year (*18*). Prompted by a possible link between Tcf4 activity and *Tcf1* expression in the intestine, we performed autopsies on *Tcf1*$^{-/-}$ mice of various ages. Unexpectedly, we observed mammary gland adenomas and polyplike intestinal neoplasms in these mice (Fig. 3A). These lesions

**Table 1.** *Min*/+*Tcf1*$^{-/-}$ mice demonstrated a 10-fold increase in the formation of intestinal neoplasms compared with *Min*/+ mice. ND, not done (mice were killed at 4 months).

| Genotype | Age (months) | No. of neoplasms in small intestine (mean ± 1 SD) | No. of neoplasms in colon (mean ± 1 SD) |
|---|---|---|---|
| Min/+Tcf1$^{+/+}$ | 3 | 9 ± 3 ($n$ = 9) | 0.5 ± 1 ($n$ = 9) |
| Min/+Tcf1$^{-/-}$ | 3 | 102 ± 10 ($n$ = 9) | 11.0 ± 3 ($n$ = 9) |
| Min/+Tcf1$^{+/+}$ | 5–6 | 35 ± 13 ($n$ = 7) | 1.1 ± 1.1 ($n$ = 7) |
| Min/+Tcf1$^{+/-}$ | 5–6 | 48 ± 15 ($n$ = 7) | 3.2 ± 2.2 ($n$ = 7) |
| Min/+Tcf1$^{-/-}$ | 5–6 | ND | ND |

[1]Department of Immunology and [2]Center for Biomedical Genetics, [3]Department of Pathology, University Medical Center Utrecht, Post Office Box 85500, 3508 GA Utrecht, Netherlands.

*These authors contributed equally to this work.
†To whom correspondence should be addressed. E-mail: h.clevers@lab.azu.nl

were never observed in littermates. Histological examination (*13*) of the intestinal and mammary gland lesions revealed typical epithelial polyps and adenoacanthomas, respectively, expressing high levels of cytoplasmic and nuclear β-catenin (Fig. 3, B and C). Significantly, the APC protein appeared absent in the intestinal adenomas (Fig. 3D).

One possible explanation for this tumor phenotype is that Tcf1 acts as a feedback transcriptional repressor of β-catenin–Tcf4 target genes and that disruption of this negative feedback loop would allow the formation of epithelial tumors much like the loss of APC. This notion predicts synergy between the loss of Tcf1 and of APC. To test this, we crossed the *Apc* allele *Multiple intestinal neoplasia (Min)* into the *Tcf1*$^{-/-}$ strain. *Min*/+ mice develop multiple polyps mostly in the small intestine (*19*). They infrequently develop extraintestinal neoplasia, notably adenoacanthomas in the mammary gland (*20*). *Min*/+*Tcf1*$^{-/-}$ mice displayed a marked enhancement of the intestinal *Min*/+ phenotype (Table 1). Adenomatous polyps were observed throughout the entire intestinal tract. Although the intestinal polyps tended to be larger than those of *Min*/+ mice, they were of similar histology and did not show any sign of tumor progression (Fig. 4A). All intestinal neoplasms that were analyzed by immunohistochemistry (stomach, small intestine, and colon) expressed high levels of β-catenin (for example Fig. 4, B and F). In addition, all females carried adenoacanthomas of the mammary gland by 8 weeks of age, while a substantial number of older male mice developed similar lesions (Table 2 and Fig. 4C). Again, the lesions typically expressed high levels of β-catenin compared with surrounding nontransformed cells (Fig. 4D). About 60% of the mice at 4 months of age had adenomas and adenoacanthomas of the sali-

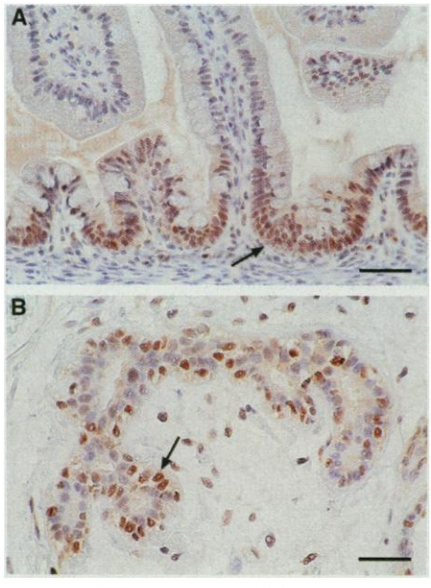


**Fig. 1.** Tcf1 is expressed in (**A**) the nucleus of fetal and adult epithelial cells of the intestine (a 16-week fetal sample is shown) and (**B**) in basal epithelial cells of the mammary gland tissue. Bars, 0.1 mm.

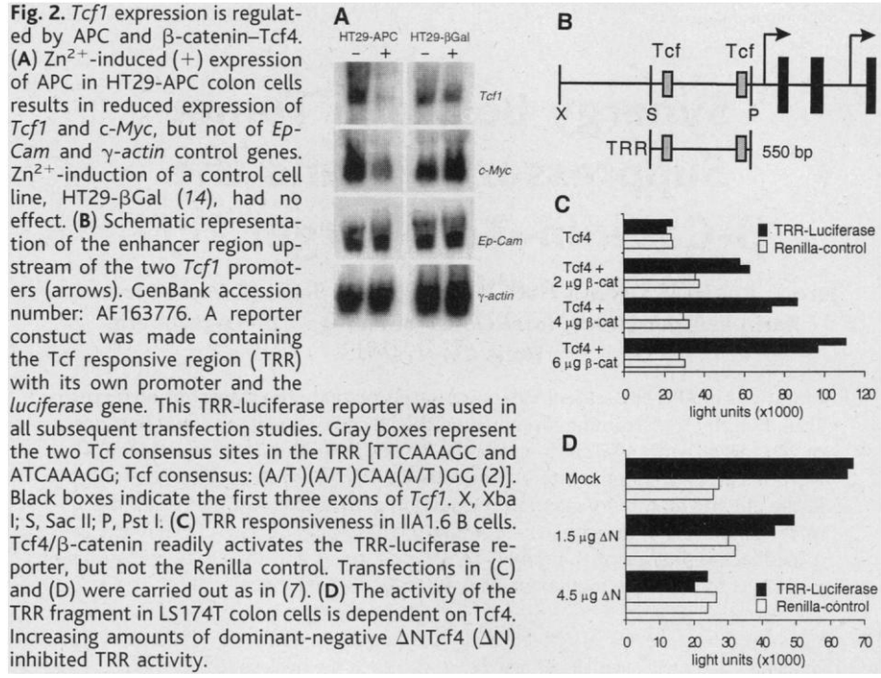


**Fig. 2.** *Tcf1* expression is regulated by APC and β-catenin–Tcf4. (**A**) $Zn^{2+}$-induced (+) expression of APC in HT29-APC colon cells results in reduced expression of *Tcf1* and c-*Myc*, but not of *Ep-Cam* and γ-*actin* control genes. $Zn^{2+}$-induction of a control cell line, HT29-βGal (*14*), had no effect. (**B**) Schematic representation of the enhancer region upstream of the two *Tcf1* promoters (arrows). GenBank accession number: AF163776. A reporter constuct was made containing the Tcf responsive region (TRR) with its own promoter and the *luciferase* gene. This TRR-luciferase reporter was used in all subsequent transfection studies. Gray boxes represent the two Tcf consensus sites in the TRR [TTCAAAGC and ATCAAAGG; Tcf consensus: (A/T)(A/T)CAA(A/T)GG (*2*)]. Black boxes indicate the first three exons of *Tcf1*. X, Xba I; S, Sac II; P, Pst I. (**C**) TRR responsiveness in IIA1.6 B cells. Tcf4/β-catenin readily activates the TRR-luciferase reporter, but not the Renilla control. Transfections in (C) and (D) were carried out as in (*7*). (**D**) The activity of the TRR fragment in LS174T colon cells is dependent on Tcf4. Increasing amounts of dominant-negative ΔNTcf4 (ΔN) inhibited TRR activity.

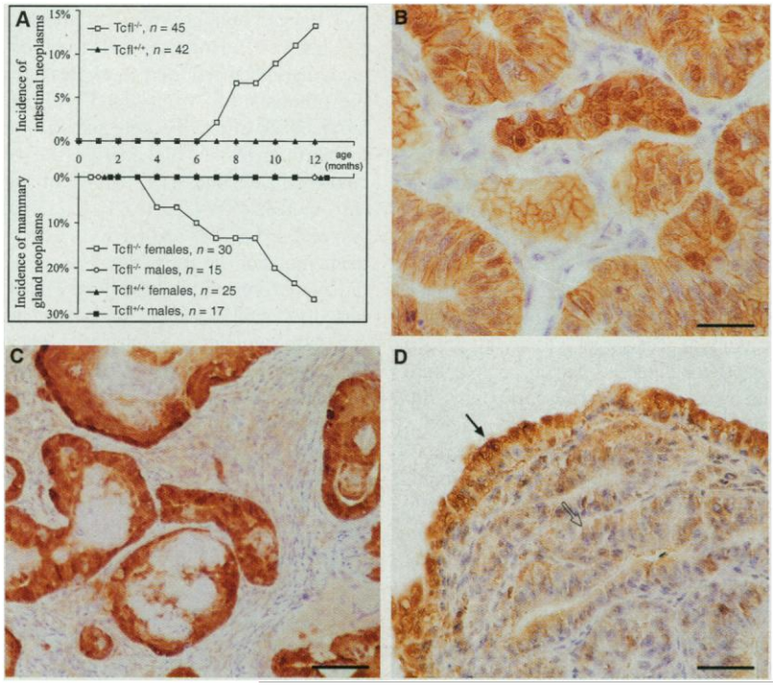


**Fig. 3.** *Tcf1*$^{-/-}$ mice develop spontaneous intestinal and mammary gland adenomas. (**A**) Fifteen percent of *Tcf1*$^{-/-}$ mice developed intestinal adenomas during the first year of life (top), whereas 25% of *Tcf1*$^{-/-}$ females developed mammary gland adenoacanthomas (bottom). (**B**) Immmmunohistological examination of spontaneous intestinal neoplasms demonstrated high levels of cytoplasmic and nuclear β-catenin. For comparison, see the nontransformed epithelium in Fig. 4, A and B. (**C**) Mammary gland lesions were typed as adenoacanthomas and found to express high levels of cytoplasmic and nuclear β-catenin. (**D**) Intestinal adenomas have lost expression of APC as analyzed by immunohistochemistry (open arrow), compared with surrounding normal epithelium (closed arrow).

vary glands (Fig. 4E). The enhanced neoplastic phenotype was not observed in *Min/+Tcf1*$^{+/-}$ littermates, ruling out any influence of genetic background. These observations reveal a strong genetic interaction between *APC* and *Tcf1*.

Insight into the nature of the genetic program activated by Tcf4 has come from a gene disruption experiment. Mice deficient in Tcf4 develop normally, but die shortly after birth due to the absence of cycling epithelial progenitor cells in the prospective crypts of the small intestine (*21*). β-catenin–Tcf4 signaling appears to activate or maintain a progenitor cell phenotype. In concordance with this, recent reports have identified c-*Myc* and *cyclinD1* as target genes of Tcf4 (*15*, *22*). Our data indicate that *Tcf1* expression in epithelial cells is similarly controlled by APC and β-catenin–Tcf4. The genetic evidence indicates that Tcf1 serves as a negative-feedback regulator in APC-related carcinogenesis. The DNA-binding HMG boxes of the four mammalian Tcf/Lef proteins are essentially identical, implying that they may regulate the same target genes (*2*). We propose a model in which the transcriptional activation of target genes such as c-*Myc* and *cyclinD1* by β-catenin–Tcf4 is counteracted by repressor isoforms of Tcf1.

It will be of interest to analyze the status of the *TCF1* locus in human breast or colon cancer. The *APC* (5q2.1) and *TCF1* (5q31.1) loci are linked in humans (*23*); large deletions on chromosome 5q could simultaneously inactivate both genes. In mice, the genes reside on separate chromosomes. *Int-1/Wnt-1* was originally cloned as a proto-oncogene activated in breast epithelium by mouse mammary tumor virus integrations (*24*). By analogy to our observations, *Int-1/Wnt-1* transgenic mice develop neoplasms in mammary glands as well as in salivary glands (*25*). In light of this observation, and given that APC functions as a regulator of Wnt signaling in a large variety of tissues, it has been surprising that APC's tumor suppressor activity appears predominantly relevant for intestinal cancer. Our data suggest that Tcf1 cooperates with APC and that the combination of the two activities is particularly important for the prevention of mammary neoplasms in mice.

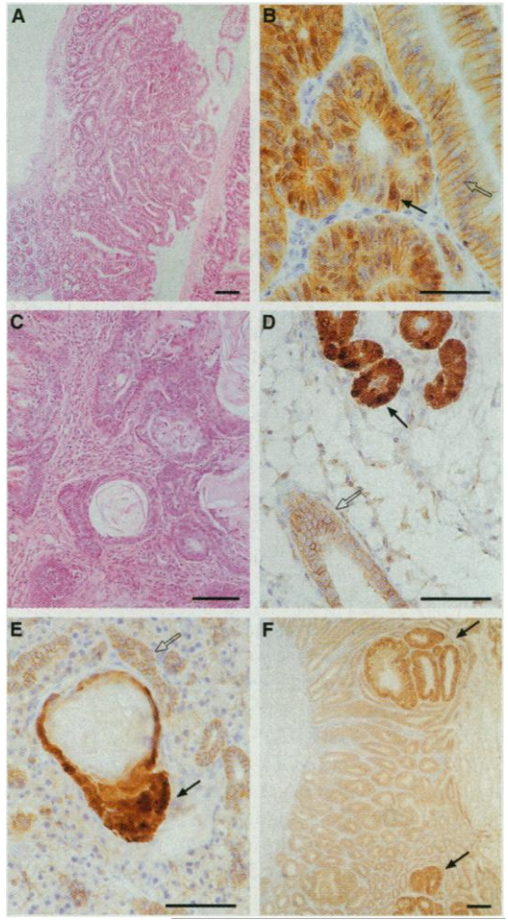


**Fig. 4.** Histology and β-catenin expression in adenomas of *Min/+Tcf1*$^{-/-}$ mice. **(A)** Polyps in the small intestine represent adenomatous lesions with moderate dysplasia, but without invasive behavior as visualized by hematoxylin and eosin stain. **(B)** High level of β-catenin expression in the polyps is revealed by immunohistochemistry (closed arrow), as compared with normal epithelium (open arrow). **(C)** A mammary gland–derived tumor showed an intimate mixture of glandular and epidermoid tissue, typical for adenoacanthomas. **(D)** Cells loaded with β-catenin in the adenoacanthoma (closed arrow) illustrate the involvement of the Wnt signal transduction pathway. Nontransformed epithelium demonstrates normal levels of β-catenin (open arrow). **(E)** In an early salivary gland adenoacanthoma and **(F)** an adenomatous lesion of the stomach, abundant nuclear β-catenin (closed arrow) illustrates the involvement of the Wnt pathway.

**Table 2.** At the age of 2 months, all *Min/+Tcf1*$^{-/-}$ females (F) developed mammary adenoacanthomas. *Min/+Tcf1*$^{-/-}$ males (M) developed the same type of adenoacanthomas, although at lower incidence. Mammary gland neoplasms did not occur in *Min/+Tcf1*$^{+/-}$ mice of either sex. Mice were killed at the indicated age.

| Genotype | Sex | Age (months) | Incidence of mammary neoplasms (%) | No. of foci per mouse (mean) |
|---|---|---|---|---|
| Min/+Tcf1$^{-/-}$ | F | 1 | 0 ($n$ = 2) | – |
| | | 2 | 100 ($n$ = 5) | 1.6 (8/5) |
| | | 3 | 100 ($n$ = 8) | 2.0 (16/8) |
| | | 4 | 100 ($n$ = 14) | 3.4 (47/14) |
| Min/+Tcf1$^{-/-}$ | M | 1 | 0 ($n$ = 4) | – |
| | | 2 | 0 ($n$ = 1) | – |
| | | 3 | 11 ($n$ = 9) | 1.0 (1/1) |
| | | 4 | 33 ($n$ = 9) | 1.0 (3/3) |
| Min/+Tcf1$^{+/-}$ | F | 5–6 | 0 ($n$ = 6) | – |
| | M | 5–6 | 0 ($n$ = 12) | – |

## References and Notes


1. About 50% of the Western population develop colorectal adenomas by the age of 70 [D. Ransohoff and C. Lang, *N. Engl. J. Med.* **325**, 37 (1991)], and at least 85% of these tumors contain *APC* mutations [Y. Miyoshi *et al.*, *Hum. Mol. Genet.* **1**, 229 (1992); J. Jen *et al.*, *Cancer Res.* **54**, 5523 (1994). Reviewed by K. Kinzler and B. Vogelstein [*Cell* **87**, 159 (1996)] and by P. Polakis [*Biochem. Biophys. Acta* **1332**, F127 (1997)].
2. K. Cadigan and R. Nusse, *Genes Dev.* **11**, 3286 (1997); H. Clevers and M. van de Wetering, *Trends Genet.* **13**, 485 (1997).
3. B. Rubinfeld *et al.*, *Science* **262**, 1731 (1993); L. Su, B. Vogelstein, K. Kinzler, *ibid.* p. 1734; B. Rubinfeld *et al.*, *ibid.* **272**, 1023 (1996); L. Zeng *et al.*, *Cell* **90**, 181 (1997); J. Behrens *et al.*, *Science* **280**, 596 (1998); C. Sakanaka, J. Weiss, L. Williams, *Proc. Natl. Acad. Sci. U.S.A.* **95**, 3020 (1998); S. Ikeda *et al.*, *EMBO J.* **17**, 1371 (1998); M. Hart *et al.*, *Curr. Biol.* **8**, 573 (1998); H. Yamamoto *et al.*, *Mol. Cell. Biol.* **18**, 2867 (1998).
4. H. Aberle *et al.*, *EMBO J.* **16**, 3797 (1997); J. Winston *et al.*, *Genes Dev.* **13**, 270 (1999); C. Liu *et al.*, *Proc. Natl. Acad. Sci. U.S.A.* **96**, 6273 (1999); M. Hart *et al.*, *Curr. Biol.* **9**, 207 (1999); E. Latres, D. Chiaur, M. Pagano, *Oncogene* **18**, 849 (1999).
5. M. Molenaar *et al.*, *Cell* **86**, 391 (1996); J. Behrens *et al.*, *Nature* **382**, 638 (1996); M. van de Wetering *et al.*, *Cell* **88**, 789, (1997).
6. J. Roose *et al.*, *Nature* **395**, 608 (1998); R. Cavallo *et al.*, *ibid.*, p. 604 (1998); L. Waltzer and M. Bienz, *ibid.*, p. 521.
7. V. Korinek *et al.*, *Science* **275**, 1784 (1997).
8. N. Barker *et al.*, *Am. J. Pathol.* **154**, 29 (1999).
9. P. J. Morin *et al.*, *Science* **275**, 1787 (1997); B. Rubinfeld *et al.*, *ibid.*, p.1790; E. Chan, U. Gat, J. McNiff, E. Fuchs, *Nature Genet.* **21**, 410 (1999).
10. J. Castrop *et al.*, *Blood* **86**, 3050 (1995); M. van de Wetering, J. Castrop, V. Korinek, H. Clevers, *Mol. Cell. Biol.* **16**, 745 (1996).
11. K. Mayer *et al.*, *Int. J. Cancer* **72**, 625 (1997).
12. M. van Beest and H. Clevers, unpublished data.
13. Immunohistochemistry was performed on formaldehyde- or Notox-fixed tissues, embedded in paraffin. Tissue slides (4 μm) were blocked for endogenous peroxidase activity by a 20-min incubation with 1.5% $H_2O_2$ in methanol. Slides were stained with antibodies to β-catenin (C19220; Transduction Labs, Lexington,

KY) and APC (C-20; Santa Cruz Biotechnology, Santa Cruz, CA). Slides stained with antibody to Tcf1 (*9*) were immersed in a 6 mM tris, 10 mM EDTA steam bath (pH 8.0) for 20 min. The primary antibody was detected with horseradish peroxidase (HRP)–conjugated rabbit antibody to mouse (anti-mouse) immunoglobulin G (IgG) or HRP-conjugated swine anti-rabbit IgG, or both (DAKO, Copenhagen, Denmark). Diaminobenzidine (DAB; Sigma) was used as substrate.

14. P. Morin, B. Vogelstein, K. Kinzler, *Proc. Natl. Acad. Sci. U.S.A.* **93**, 7950 (1996).
15. T.-C. He *et al.*, *Science* **281**, 1509 (1998).
16. Transfections in IIA1.6 B cells were carried out as in (*7*), with 1 μg of TRR-luciferase reporter, 2 μg of hTcf4, and 0, 2, 4, or 6 μg of β-catenin–encoding plasmids. pCDNA was used to bring the total amount to 9 μg of plasmid DNA. Fifty nanograms of a cytomegalovirus promoter–Renilla plasmid was added as an internal control to monitor transfection. LS174T cells were transfected by Fugene 6 (Boehringer Mannheim, Mannheim, Germany). TRR-luciferase reporter (0.5 μg) and 0, 1.5, or 4.5 μg of ΔNTcf4-encoding plasmids were used.
17. S. Verbeek *et al.*, *Nature* **374**, 70 (1995).
18. M. Schilham *et al.*, *J. Immunol.* **161**, 3984 (1998).
19. A. Moser, H. Pitot, W. Dove, *Science* **247**, 322 (1990); L. Su *et al.*, *ibid.* **256**, 668 (1992).
20. A. Moser *et al.*, *Proc. Natl. Acad. Sci. U.S.A.* **90**, 8977 (1993); A. Moser *et al.*, *Eur. J. Cancer* **31A**, 1061 (1995).
21. V. Korinek *et al.*, *Nature Genet.* **19**, 379 (1998).
22. O. Tetsu and F. McCormick, *Nature* **398**, 422 (1999).
23. J. Groden *et al.*, *Cell* **66**, 589 (1991); I. Nishisho *et al.*, *Science* **253**, 665 (1991); M. van de Wetering *et al.*, *J. Biol. Chem.* **267**, 8530 (1992).
24. R. Nusse and H. Varmus, *Cell* **31**, 99 (1982); R. Nusse *et al.*, *Nature* **307**, 131 (1984).
25. A. Tsukamoto *et al.*, *Cell*, **55** 619 (1988).
26. We thank the Department of Pathology and the Audio-Visual Center for support, K. Kinzler for the HT-29 cell lines, and R. Fodde and colleagues for helpful discussions.

6 July 1999; accepted 19 August 1999

# Antiangiogenic Activity of the Cleaved Conformation of the Serpin Antithrombin

**Michael S. O'Reilly,[1,3]* Steven Pirie-Shepherd,[1] William S. Lane,[2] Judah Folkman[1]**

**Antithrombin, a member of the serpin family, functions as an inhibitor of thrombin and other enzymes. Cleavage of the carboxyl-terminal loop of antithrombin induces a conformational change in the molecule. Here it is shown that the cleaved conformation of antithrombin has potent antiangiogenic and antitumor activity in mouse models. The latent form of intact antithrombin, which is similar in conformation to the cleaved molecule, also inhibited angiogenesis and tumor growth. These data provide further evidence that the clotting and fibrinolytic pathways are directly involved in the regulation of angiogenesis.**

For a carcinoma to expand beyond a prevascular size, it must produce stimulators of angiogenesis in excess of inhibitors (*1*, *2*), and the continued production of the inhibitors provides one mechanism for the inhibition of tumor growth by tumor mass (*3*, *4*). Using murine models, we identified the angiogenesis inhibitors angiostatin (*3*) and endostatin (*4*). To determine if human tumors produce similar inhibitors, we screened small-cell lung cancer cell lines for their ability, when grown on a mouse flank, to inhibit the growth of a comparable implant on the opposite flank. We chose small-cell lung cancer because, clinically, metastases can grow rapidly after treatment of primary disease. One cell line, NCI-H69, inhibited the growth of a secondary implant by 80%. By selective in vivo passage, variants of this line were developed. In one variant, H69i, the inhibition of one tumor by the other was virtually 100% (Fig. 1A). In a second, H69ni, there was no inhibition (Fig. 1B).

Using a 72-hour proliferation assay (*4*), we detected an inhibitor of endothelial cell proliferation in conditioned media of the H69i cell line. The activity was purified (*5*) to apparent homogeneity, eluted at 54 to 56% acetonitrile from a C4 high-performance liquid chromatography (HPLC) column, and was associated with a 58-kD band that migrated as two bands of 53 to 55 kD and 3 to 5 kD under reducing conditions. The inhibitory band initially copurified with one that migrated (reduced) at 58 to 60 kD (Fig. 1C). $NH_2$-terminal microsequence analysis revealed identity to bovine antithrombin (Fig. 2). Microsequence analysis of both the 53- to 55-kD and the 3- to 5-kD band revealed that the inhibitory protein is cleaved bovine antithrombin (Fig. 2). The cleavage site between $Ser^{386}$ and $Thr^{387}$ has not previously been described. Enzymes that cleave antithrombin include thrombin ($Arg^{394}$-$Ser^{395}$) and pancreatic ($Val^{388}$-$Iso^{389}$) and human neutrophil elastase ($Iso^{391}$-$Ala^{392}$) (*6*, *7*). Conditioned media from the H69ni cells did not substantially inhibit endothelial cell proliferation even when applied to heparin Sepharose with a protocol similar to that described (*8*). These data strongly suggest that the inhibition of angiogenesis by cleaved antithrombin from the H69i cells is in part responsible for the inhibition of tumor growth observed in vivo.

Antithrombin circulates in a quiescent form in which its reactive COOH-terminal loop is not fully exposed and cannot bind target proteases. Heparin induces a stressed conformation of the molecule, exposes the reactive loop (*6*, *9*), and increases thrombin affinity by up to a factor of 100 (*6*). The thrombin-antithrombin complex can slowly dissociate, and the reactive loop of antithrombin is cleaved by the released thrombin (*10*, *11*). Cleaved antithrombin consists of disulfide-bonded A and B chains and does not bind target proteases. Cleavage induces a conformational change to a relaxed (R) form in which the loop irreversibly inserts into the A-beta sheet (*12*). A similar irreversible conformational change of antithrombin to a latent form has been described (*13*, *14*). Mild denaturation of the molecule (*13*) induces a locked conformation characterized by polymers of the latent molecule, and heat treatment with citrate produces a latent monomeric antithrombin (*14*).

Cleaved antithrombin was purified from bovine calf serum (*15*), and human antithrombin was purified from outdated plasma (*15*) and cleaved with pancreatic elastase (*16*). The cleaved antithrombin potently inhibited endothelial cell proliferation induced by bovine fibroblast growth factor (Fig. 3) or by vascular endothelial growth factor (*8*) in a dose-dependent fashion with half-maximal inhibition seen at 50 to 100 ng/ml. The stressed conformation of antithrombin had no substantial effect on capillary endothelial cell proliferation at comparable doses (Fig. 3) but did show marginal inhibition at doses in excess of 5 μg/ml.

To produce the locked conformation (*13*), we incubated antithrombin in 0.9 M guanidine and then performed dialysis. Monomeric latent human antithrombin was produced as described by incubating stressed antithrombin (0.5 mg/ml) in 0.25 M trisodium citrate and 10 mM tris-HCl (pH 7.4) at 60°C for 18 hours (*14*). Both potently inhibited capillary endothelial cell proliferation in a dose-dependent and reversible fashion with half-maximal inhibition observed at 50 to 100 ng/ml (*8*). These data demonstrate that the conformational change that occurs after cleavage of antithrombin confers antiangiogenic activity, and we refer to this conformation as antiangiogenic antithrombin (aaAT).

[1]Department of Surgery, Children's Hospital, Departments of Surgery and Cellular Biology, [2]Harvard Microchemistry Facility, 16 Divinity Avenue, Cambridge, MA 02138, USA. [3]Joint Center for Radiation Therapy, Harvard Medical School, 300 Longwood Avenue, Boston, MA 02115, USA.

*To whom correspondence should be addressed. E-mail: oreilly@hub.tch.harvard.edu